J Electroceram (2009) 23:37–42
DOI 10.1007/s10832-008-9517-z

# Synthesis of $(Ba_{0.5}Sr_{0.5})(Ti_{1-x}Zr_x)O_3$ ceramics: Effect of Zr content on room temperature electrical properties

**S. K. Rout · P. K. Barhai · S. Panigrahi · I. W. Kim**

Received: 6 September 2007 / Accepted: 24 April 2008 / Published online: 17 May 2008


**Abstract** The phase formation behavior and room temperature dielectric properties of bulk perovskite solid solution composition $(Ba_{0.5}Sr_{0.5})(Ti_{1-x}Zr_x)O_3$ have been investigated. The samples with different Zr-content were prepared through solid state reaction. The XRD investigation showed that $Zr^{+4}$ is systematically dissolved in $Ba_{0.5}Sr_{0.5}TiO_3$ lattice up to about 60 atm.% substitution, having cubic *Pm3m* structure. Eighty atom percent Zr substituted composition showed to contain a cubic phase similar to that of $x=0.6$ composition and a tetragonal (*I*4/*mcm*) phase. That is the solid solution breaks around at 80 atm.% Zr substitutions. $Ba_{0.5}Sr_{0.5}ZrO_3$ was having orthorhombic *Imma* structure. Decrease in grain sizes were observed with increase in Zr content. The permittivity of the ceramics decreased with the increase in Zr substitution. The frequency dependency of dielectric loss in the frequency range 10 Hz to 10 MHz, were improved with Zr substitution in the ceramics. The room temperature ac and dc conductivity also decreased significantly with the increase in Zr-content.

S. K. Rout (✉) · P. K. Barhai
Department of Applied Physics, BIT, Mesra,
Ranchi Pin-835 215, India
e-mail: skrout@bitmesra.ac.in

S. Panigrahi
Department of Physics, National Institute of Technology,
Rourkela 769 008, India

I. W. Kim
Department of Physics, University of Ulsan,
Ulsan, South Korea

*Present address:*
S. K. Rout
Department of Chemical and Biomolecular Engineering, KAIST,
Daejeon, South Korea

**Keywords** Electronic ceramics · Dielectric properties · Barium-strontium titanate-zirconate

## 1 Introduction

The Barium Strontium Titanate (BST) has been considered to be an important material for tunable microwave devices as well as dynamic random access memory (DRAM) applications because of its high dielectric constant, large electric field tunability, relatively low dielectric loss and variable Curie temperature from 30 to 400 K depending on the composition of barium [1–5]. The recent work [6] suggests that $Ba_{1-x}Sr_xTiO_3$ thin films with $x=0.5$–$0.6$ are preferred for use at room temperature tunable circuit components. For example, it is reported [7] that a strong bias voltage tunability and very low hysteresis in the composition $Ba_{0.5}Sr_{0.5}TiO_3$. Considering all these, the compositions $Ba_{0.5}Sr_{0.5}TiO_3$ has been selected as a base material in the present study to investigate the effect of $Zr^{4+}$ substitution for $Ti^{4+}$ in the material.

This substitution was planned as, it is reported that the substitution of $Ti^{4+}$ with $Zr^{4+}$ ions in barium titanate can reduce the dielectric loss or leakage current in the material [8]. Moreover, the $Zr^{4+}$ ion is chemically more stable than the $Ti^{4+}$ and has a larger ionic size to expand the perovskite lattice. Therefore the conduction by electron hopping between $Ti^{4+}$ and $Ti^{3+}$, if any, would be depressed by the substitution of Ti with Zr. The BST thin films often have high current emission at low electric field [9]. Therefore, new types of dielectrics with high dielectric constant and low stable leakage current need to be developed. It is expected that Zr-doped $Ba_{0.5}Sr_{0.5}TiO_3$ ceramics should have further improved dielectric losses. A high dielectric constant and low leakage current of

$(Ba_{0.65}Sr_{0.35})(Ti_{0.65}Zr_{0.35})O_3$ thin film has been reported [10] and proposed as a promising material for DRAM applications. A similar type of compositionally graded multilayer $(Ba_{0.8}Sr_{0.2})(Ti_{1-x}Zr_x)O_3$ films have shown an improved dielectric properties and tunability [5]. The tenability of $(Ba_{0.85}Sr_{0.15})(Ti_{0.82}Zr_{0.18})O_3$ thin films has been reported 57% at an applied voltage of 415 kV/cm [11]. However, no literature are available on phase formation and dielectric properties of typical bulk $(Ba_{0.5}Sr_{0.5})(Ti_{1-x}Zr_x)O_3$ ceramics. In this work, a study concerning the phase formation behaviour, room temperature dielectric properties and conduction characteristic of bulk $(Ba_{0.5}Sr_{0.5})(Ti_{1-x}Zr_x)O_3$ ceramics is reported. Voltage tunability characteristics of the different compositions will be reported separately.

## 2 Experimental

The samples were prepared through solid state reaction route. The compositions with different value of $x$ (=0.2, 0.4, 0.5, 0.6, 0.8, and 1.0) in $(Ba_{0.5}Sr_{0.5})(Ti_{1-x}Zr_x)O_3$ is prepared from $BaCO_3$ (S.D. Fine Chem., Mumbai), $SrCO_3$ (S.D. Fine Chem., Mumbai), $TiO_2$ (E. Merck India Ltd.) and $ZrO_2$ (Loba Chem., Mumbai). All the powders were having more than 99% purity. Particle size of starting raw materials, measured using Malvern Mastersizer, were: $SrCO_3$ [$D(v,0.1)$=0.48 μm, $D(v,0.5)$=13.13 μm, $D(v,0.9)$= 24.63 μm], $BaCO_3$ [$D(v,0.1)$=0.25 μm, $D(v,0.5)$=2.09 μm, $D(v,0.9)$=13.20 μm], $TiO_2$ [$D(v,0.1)$=0.27 μm, $D(v,0.5)$= 0.35 μm, $D(v,0.9)$=0.48 μm] and $ZrO_2$ [$D(v,0.1)$=0.42 μm, $D(v,0.5)$=10.27 μm, $D(v,0.9)$=15.48 μm]. The powders were thoroughly mixed in agate mortar using isopropyl alcohol. The homogenous mixtures were calcined at 1300 °C for 4 h, 1400 °C for 4 h and finally 1500 °C for 4 h with intermediate mixing and grinding between each firing. The calcined powders were characterized with respect to phase identification and lattice parameter measurement, all by using Cu-$K_\alpha$ XRD (PW-1830, Philips, Netherlands).

For electrical property measurements, the disks were pressed uniaxially at 200 Mpa with 2 wt% PVA solution added as binder and these were sintered at 1500 °C for 1 h. Disk density was determined using Archimedes principle. True porosity was calculated using X-ray density calculated from lattice parameters. Average grain sizes were measured by an optical microscope. For electrical measurement silver electrodes were printed on to opposite faces of the disk and were sintered at 700 °C for 15 min. Room temperature dielectric measurements were carried out over range 10 Hz to 13 MHz using HP-4192A LF Impedance Analyzer. Dielectric conductivity of the samples was calculated using capacitance and tanδ values measured at 100 kHz, 500 kHz and 1 MHz. Room temperature d.c. conductivity of the samples was studied with a Keithley-237 electrometer (Keithley Instruments, Inc., USA).

Prior to the measurement, a poling voltage of +10V were applied for 10s in order that the domains align along the preferred orientation. After initializing the polarization state, and waiting for 20s, the static current is measured by applying a dc bias from 0V to 100V in step of 1V at room temperature. The static current in this measurement is non switching, meaning that the capacitor remain in the state of positive polarization prior to the measurement. DC conductivity was calculated using the standard procedure. The following parameters in this measurement are important; (a) the magnitude and duration of the poling voltage, (b) wait time, from the ending of the poling voltage to the beginning of the current measurement, (c) delay time, between the application of each voltage step and the current measurement and (d) integrated mode of the measurement.

## 3 Results and discussion

Figure 1 shows the XRD pattern of $(Ba_{0.5}Sr_{0.5})(Ti_{1-x}Zr_x)O_3$ ceramics with different $x$ value. It is evident from the figure that all the peaks correspond to perovskite phase. The XRD patterns were indexed and cell parameters were refined using standard CCP-14 program "CHEKCELL" [http://www.ccp14.ac.uk/tutorial/1mgp/]. The composition with $x$=0 was indexed in cubic system and was similar to PDF-2 card no. 39-1395 for the material $Ba_{0.5}Sr_{0.5}TiO_3$. The intermediate compositions from $x$=0.2 to 0.6, were also indexed in cubic system with space group symmetry *Pm3m*. The diffraction pattern of $x$=0.8 composition was analyzed to contain cubic and tetragonal (*I*4/*mcm*) phase mixture. The cubic phase of $x$=0.8 composition was very

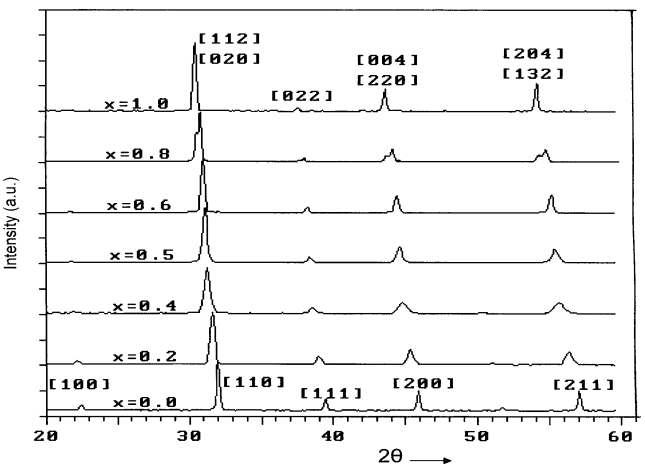


**Fig. 1** XRD pattern of $(Ba_{0.5}Sr_{0.5})(Ti_{1-x}Zr_x)O_3$ ceramics with their representative value of $x$ (Zr) in the composition. Indexing (cubic) in $x$=0.0 is valid up to $x$=0.6, orthorhombic for $x$=1.0 and $x$=0.8 is mixed phase of the both

similar to the cubic phase of $x$=0.6 composition. This indicates that solid solution breaks around the composition $x$=0.8. The 80 atm.% Zr substituted composition also suggests having super lattice structure due to the presence of two dissimilar structures [7].

The end composition with $x$=1.0, i.e. $Ba_{0.5}Sr_{0.5}ZrO_3$, was indexed in orthorhombic *Imma* system [12]. No standard XRD pattern is available in PDF-2 data file for barium strontium zirconate ($x$=1.0) material. We may take it as a general rule that distortion of the unit cell which decreases its symmetry introduces additional variable parameters and increases the number of lines on the diffraction pattern [13]. Of course, the position of these diffraction peaks depends up on the unit cell volume.

It can be seen from the XRD pattern that the most prominent reflection of $Ba_{0.5}Sr_{0.5}TiO_3$ composition near $2\theta$ ~32° was indexed as [110] reflection of cubic symmetry and the diffraction peak near $2\theta$~30.5° of $Ba_{0.5}Sr_{0.5}ZrO_3$ composition was indexed as overlapping [020] and [112] reflection of orthorhombic symmetry. The highest intensity peak of the compositions containing 80% of Zr, i.e $Ba_{0.5}Sr_{0.5}$ $(Ti_{0.2}Zr_{0.8})$ $O_3$ was indexed as [110] reflection of cubic and [002] reflection of tetragonal symmetry. These identifications reveled that the system ($Ba_{0.5}Sr_{0.5}TiO_3$) transform from cubic to orthorhombic ($Ba_{0.5}Sr_{0.5}ZrO_3$) upon Zr substitution for Ti, through an intermediate tetragonal phase formation. Changes of this nature are not uncommon among phase transformations and ordering reactions [12]. Similar sequence in fact, orthorhombic (*Imma*) → tetragonal (*I*4/*mcm*) → cubic (*Pm3m*) have been observed by Kennedy et. al. [12], in $Sr_{1-x}Ba_xZrO_3$ ceramics after a high resolution X-ray diffraction study. Similar type of structural transformation was also studied by the author and reported [14]. In general we proposed the symmetry of the intermediate compounds based on the observation of resolved splitting or asymmetry in the appropriate reflections and/or the observation of the weak superlattice reflections that are diagnostic of the space group. In the present compounds the extremely strong X-ray scattering power of the heavy Ba and Zr atoms often made it difficult to detect those weak super lattice reflections that arise from displacement of the light O atoms. In all cases the structures were assigned to the highest possible symmetry that fully accounted for the observed data. In the present case the composition steps are comparatively coarse. Nevertheless, the same phenomena appear; that is, continuous transition from *Pm3m* to *I*4/*mcm* and the first-order transition from *I*4/*mcm to Imma* as reported by Kennedy et. al. [12]. The detailed crystallographic information is reported elsewhere [15] after Rietveld refinement. The Fig. 1 also shows that the substitution of $Zr^{4+}$ for $Ti^{4+}$ increases the d-spacing yielding the shift of diffraction peaks towards lower $2\theta$ angle. This is the clear indication that $Zr^{4+}$ is systematically dissolved in $Ba_{0.5}Sr_{0.5}TiO_3$ lattice up to 60 atm.% substitutions. Lattice parameter increases due to the incorporation of bigger $Zr^{4+}$ (0.087 nm) for smaller $Ti^{4+}$ (0.068 nm).

The lattice parameters of respective cubic, tetragonal and orthorhombic phases present in the samples are shown in the Table 1, along with the full width at half maxima (FWHM) of the 100% relative intensity ($I_{100}$) peak of the phases. Composition with $x$=0.2, 0.4 and 0.5 shows comparatively higher FWHM (Table 1) than other samples. The peak broadening can arise in a number of ways including compositional inhomogeneity, hysteresis near the phase transition, presence of defects in the crystal lattice, presence of very fine particles, etc. The presence of very fine particles may be ruled out here because of the several heat treatments during processing. For example the composition $x$=0.2 shows a high FWHM, although it was all most melted during high temperature calcination. Here the

**Table 1** The crystal symmetry, lattice parameter, FWHM of 100% relative intensity peak of the phases present, grain size, X-ray density, experimental density and apparent porosity in the $(Ba_{0.5}Sr_{0.5})(Ti_{1-x}Zr_x)O_3$ system with different Zr ($x$) concentration.

| Zr ($x$) | Symmetry | Lattice parameter | FWHM of $I_{100}$ peak | Grain size (μm) | X-ray density (gm/cc) | Bulk density (gm/cc) | Apparent porosity (%) |
|---|---|---|---|---|---|---|---|
| 0 | Cubic(*Pm3m*) | $a_0$=3.9535(12) | 0.114 | 21.1 | 5.596 | 5.343 | 1.15 |
| 0.2 | Cubic | $a_0$=4.0046(41) | 0.302 | 19.8 | 5.6107 | 5.298 | 2.25 |
| 0.4 | Cubic | $a_0$=4.0485(40) | 0.415 | 11.6 | 5.6471 | 5.156 | 4.8 |
| 0.5 | Cubic | $a_0$=4.0725(19) | 0.260 | 7.3 | 5.7194 | 4.971 | 6.46 |
| 0.6 | Cubic | $a_0$=4.0822(11) | 0.156 | 5.1 | 5.7199 | 4.895 | 7.4 |
| 0.8 | Cubic (pm3m) + | $a_0$=4.1076(17) | 0.185 | 4.1 | 5.8128 | 4.84 | 8.2 |
| | tetragonal (*I*4/*mcm*) | $a_0$=5.8707(80) | 0.219 | | 5.7332 | | |
| | | $c_0$=8.1683(44) | | | | | |
| 1.0 | Orthorhombic (*Imma)* | $a_0$=5.8855(22) | 0.121 | 2.5 | 5.8122 | 4.842 | 8.25 |
| | | $b_0$=8.2924(33) | | | | | |
| | | $c_0$=5.8852(11) | | | | | |

associated broadening may be related to the formation of disorder cubic structure as reported [16] for barium titanate zirconate (BZT). This disorderness (i.e. peak broadening) is maximum at $x$=0.4 composition.

Figure 2 shows the effect of Zr ($x$) on microstructure of $(Ba_{0.5}Sr_{0.5})Ti_{1-x}Zr_xO_3$ceramics. There is a decrease in average grain size with the increase in Zr ($x$) content. The decreasing grain size with increasing Zr content may be attributed to lower grain growth rates from the slower diffusion of $Zr^{4+}$ ion, which has a bigger ionic radius than $Ti^{4+}$ and $Zr^{4+}$ ion is also chemically more stable than $Ti^{4+}$ ion. Crystallization may be initiated earlier with lower Zr contents, resulting in a larger grain size for the same heat treatment. The decrease in grain size in Zr may also imply that the existence of Zr in BST ceramic makes the initiation of crystallization harder to occur. The detail information on grain size with Zr content is given in the Table 1.

From the Table 1, the X-ray density of the compositions is found to increase with Zr content, may be due to the higher density of Zr (5.85 gm/cc) than that of Ti (4.5 gm/cc). But the experimental bulk density is found to decrease with Zr content. The reason may be due to increase of more stable and bigger $Zr^{4+}$ ion than $Ti^{4+}$ which reduces the initiation of grain growth (Fig. 2) at the experimental sintering temperature as well as density. As there is a large difference between their melting temperatures, a large difference in grain size is observed. Again due to this high melting temperature difference a large difference in density and porosity between the two end compositions of the series is also observed.

As the samples were having different porosities (Table 1), to compare their room temperature dielectric properties the experimental permittivity data were corrected as per the following relation.

$$\text{Actual}(\varepsilon') = \frac{\text{Experimental}(\varepsilon')}{\left(1 - \text{True Porosity}\right)}$$

The change in permittivity with frequency of $(Ba_{0.5}Sr_{0.5})(Ti_{1-x}Zr_x)O_3$ is plotted in the Fig. 3 after considering the above correction for different compositions. The permittivity ($\varepsilon$) decreases with the increase in Zr substitution due to the (1) decrease in concentration of high permittivity BST material and (2) due to the decrease in grain size hence polarizability of the atoms in the structure. For all the compositions, dielectric constant decreases nominally up to about 10–50 kHz. This is mainly due to the decrease in the space charge polarization contribution. Permittivities are stable in the frequency range 100 kHz to about 3 MHz for compositions up to $x$=0.4 and stable up to about 10 MHz for compositions with '$x$' from 0.5 to 1.0. So it may be concluded that the materials with high Zr content are suitable for high frequency application compared to BST.

Figure 4 shows the frequency dependency of the dielectric loss in the material. The high losses at lower frequency range are due to the space charge polarization relaxation losses. It is observed that the compositions with $x$=0.0 to 0.4 show low loss in the range ~100 kHz to 6–7 MHz, may be primarily due to their higher density. However, the compositions with $x$=0.5 to 1.0 have low losses in the higher frequency range ~3 MHz to 13 MHz. That is high frequency loss decreases with Zr substitution. A dispersion of loss occurs in MHz range and that loss seems to decrease with the increase in Zr content. It is

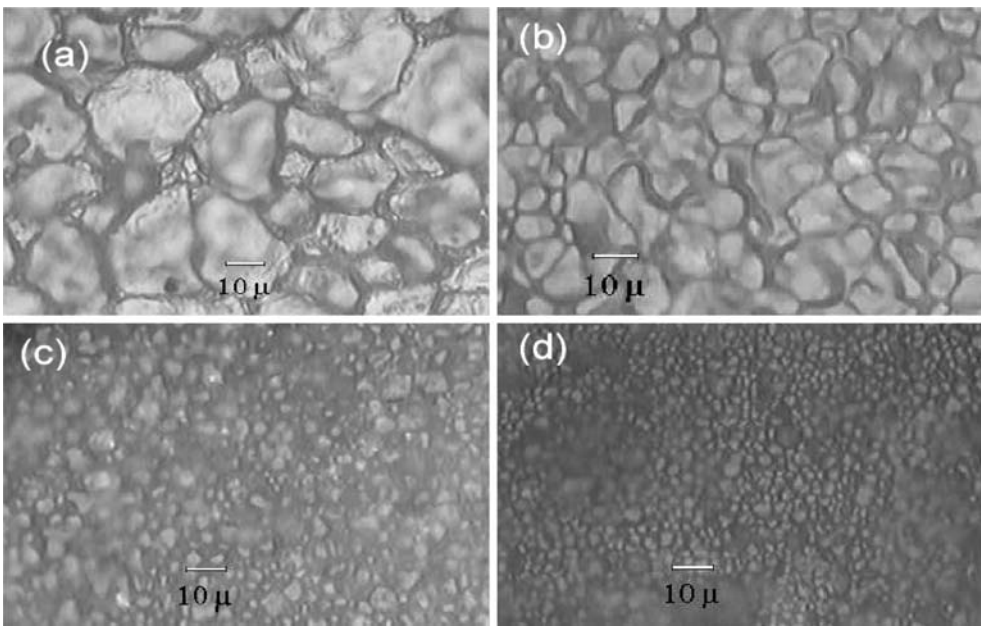


**Fig. 2** Microstructure of $(Ba_{0.5}Sr_{0.5})$ $Ti_{1-x}Zr_xO_3$ ceramics sintered at 1500 °C for 1 h, (**a**) $x$=0.0, (**b**) $x$=0.4, (**c**) $x$=0.8, and (**d**) $x$=1.0

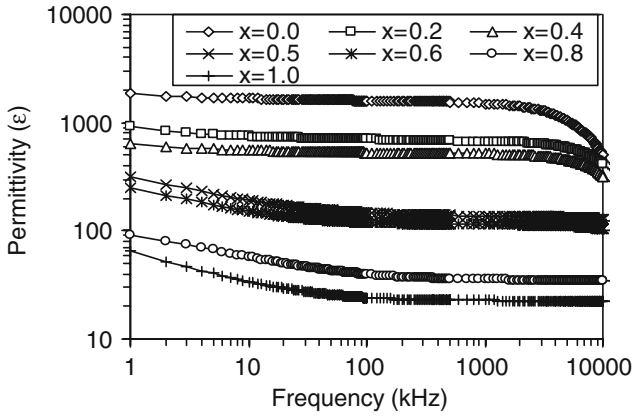


**Fig. 3** Frequency dependency of permittivity for $(Ba_{0.5}Sr_{0.5})(Ti_{1-x}Zr_x)O_3$ with different $x$ values

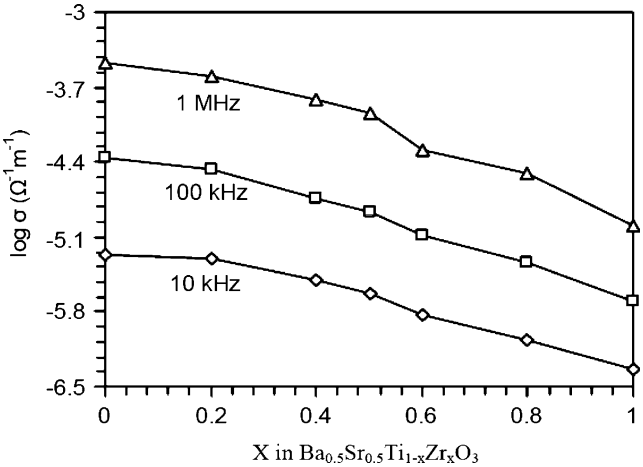


**Fig. 5** The room temperature dielectric conductivity of different $(Ba_{0.5}Sr_{0.5})(Ti_{1-x}Zr_x)O_3$ compositions

known that the increase of loss is due to the extrinsic resonance behavior [16]. Decrease in that resonance loss with Zr substitution may be considered due to the decrease in defects (vacancy, mobile ions or leaky grain boundary [17], etc.).

The room temperature dielectric conductivity (σ) of the material was evaluated at 100 kHz, 500 kHz, and 1 MHz using the formula $\sigma=(2\pi fCd \tan \delta)/A$. Where '$f$' is the operating frequency, '$d$' the thickness of the disk, '$A$' the area of the electrode, '$C$' the capacitance and 'tan $\delta$' the dielectric loss. The variation of conductivity of $(Ba_{0.5}Sr_{0.5})(Ti_{1-x}Zr_x)O_3$ compositions with Zr content is plotted in the Fig. 5. It shows that the conductivity of BST decreases rapidly with Zr substitution for Ti. It is not surprising, as it is calculated from the value of observed capacitance and dielectric loss, those decreases with increase in Zr content.

For thorough analysis of the electrical properties, d.c conductivity were calculated and presented in the Fig. 6. The figure shows the dc conductivity also decreases with Zr substitution up to $x=0.6$ in $Ba_{0.5}Sr_{0.5}Ti_{1-x}Zr_xO_3$ ceramic. The composition with $x=0.8$ and $x=1.0$ shows a small increase in conductivity may be due to the presence of mixed phase and transformation of lower symmetry orthorhombic structure.

It has been established [18] that introduction of $Zr^{+4}$ ions in $BaTiO_3$ lattice occurs in three steps; firstly filling $Ba^{+2}$ vacancies, secondly solid solution formation in between BT and BZ, thirdly occupying interstitial site in BT lattice. The reduction in conductivity of composition with increase in "$x$" may be due to the filling of $Ba^{+2}$ vacancies by the $Zr^{+4}$ ions and associated reduction in $Ba^{+2}$ vacancy induced conductivity. The end composition BSZ has lower conductivity than other end member BST, may be due to the presence of more stable $Zr^{+4}$ ions in BSZ than $Ti^{+4}$ ions in BST. The conductivity of BST is highest due to the both A-site vacancy as well as the conductivity by electron hopping between $Ti^{+4}$ and $Ti^{+3}$ ions [8].

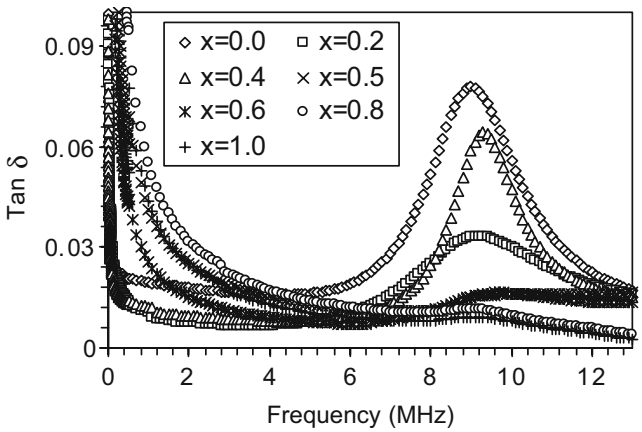


**Fig. 4** Frequency dependency of dielectric loss for different $(Ba_{0.5}Sr_{0.5})(Ti_{1-x}Zr_x)O_3$ compositions

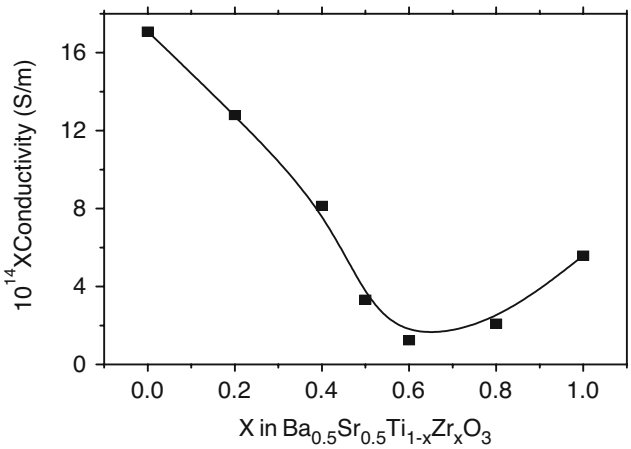


**Fig. 6** The room temperature d.c. conductivity of different $(Ba_{0.5}Sr_{0.5})(Ti_{1-x}Zr_x)O_3$ compositions

## 4 Conclusions

It may be concluded that;

1. The solid solution system $(Ba_{0.5}Sr_{0.5})(Ti_{1-x}Zr_x)O_3$ remains cubic up to $x \leq 0.6$ and the solid solution breaks around $x=0.8$ with the formation of second phase of tetragonal type. The $Ba_{0.5}Sr_{0.5}ZrO_3$ has orthorhombic structure.
2. Composition with $x=0.2$, 0.4 and 0.5 have deformed cubic structure with broadened diffraction pattern.
3. Compositions with $x=0.8$ contains both the cubic and tetragonal phases and suggesting to have superlattice structure due to the presence of two dissimilar structures.
4. Decrease ingrain size is observed due to the substitution of higher stable Zr in place of Ti on BST ceramics.
5. Permittivity, dielectric loss and conductivity decreases with Zr-substitution due to the decrease in charge defects by the substitution.

## References


1. A.T. Findikoglu, Q.X. Jia, X.D. Wu, G.J. Chen, T. Venkatesan, D. W. Reagor, Appl. Phy. Lett. **68**(5), 1651 (1996)
2. O.G. Vendik, S.P. Zubko, J. Appl. Phys. **88**, 5343 (2000)
3. U. Syamaprasad, R.K. Galgali, B.C. Mohanty, Mater. Lett. **7**, 197–200 (1988)
4. A.T. Findikoglu, R. Camassa, G. Lythe, Q.X. Jia, Appl. Phy. Lett. **80**, 3391 (1996)
5. C. Wang, B.L. Cheng, S.Y. Wang, H.B. Lu, Y.L. Zhou, Z.N. Chen, G.Z. Yang, Appl. Phys. Lett. **84**, 765–767 (2004)
6. W.J. Kim, H.D. Wu, W. Chang, S.B. Qadri, J.M. Pond, S.W. Kirchoefer, B.D. Chrisey, J.S. Horwitz, J. Appl. Phys. **88**, 5448 (2000)
7. H.M. Cristen, L.A. Knauss, K.S. Harshavardhan, Mater. Sci. Eng. B **56**, 200–203 (1998)
8. T.B. Wu, C.M. Wu, M.L. Chen, Appl. Phys. Lett. **69**, 2659–2661 (1996)
9. K. Numata, Y. Fukuda, K. Aoki, A. Nishimura, Jap. J. Appl. Phys. **34**, 5245–5249 (1995)
10. J.-D. Byun, J.-I.I. Yoon, S. Nahm, J.-C. Kim, Mater. Res. Bull. **35**, 1755–1761 (2000)
11. J. Zhai, X. Yao, H. Chen, Ceram. Int. **30**, 1237–1240 (2004)
12. B.J. Kennedy, C.J. Howard, G.J. Thorogood, J.R. Hester, J. Solid State Chem. **161**, 106–112 (2001)
13. B.D. Cullity, *Elements of X-ray Diffraction*, 2nd edn. (Addison-Wesley, Reading, MA, 1978)
14. J. Bera, S.K. Rout, J. Electroceram, **18**, 33–37 (2007)
15. S.K. Rout, Phase formation and dielectric study on BaO-$TiO_2$-$ZrO_2$ perovskite system, Ph. D thesis, Dept of Physics, NIT, Rourkela, (2006)
16. A. Dixit, S.B. Majumdar, P.S. Dobal, R.S. Katiyar, A.S. Bhalla, Thin Solid Films **447–448**, 284–288 (2004)
17. L.I. Maissel, R. Glang, *Handbook of Thin Film Technology* (McGraw-Hill, New York, 1970)(Chapter 16)
18. F.M. Pontes, E. Longo, E.R. Leite, J.A. Varela, Thin Solid Films **386**, 91–98 (2001)